omnidoc.top

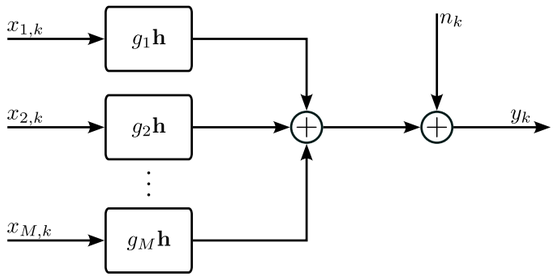


Figure 1: Block diagram of a complex-valued MISO system.

and its structure heavily depends on the application at hand. Likewise, the physical interpretation of the parameter vectors $\mathbf{h}$ and $\mathbf{g}$ is very application-dependent. As an introductory toy example, the input–output relation of the complex-valued MISO system in Figure 1 can be written in the form of (3). This model is valid when each channel impulse response is a scaled copy of a common impulse response $\mathbf{h}$. With M input signals $x_{m,k}$ in combination with M linear channels $g_m\mathbf{h} \in \mathbb{C}^L$, for $m = 1, \ldots, M$, the input signal matrix is defined as

$$\mathbf{X}_k = \begin{bmatrix} \mathbf{x}_{1,k} & \cdots & \mathbf{x}_{M,k} \end{bmatrix}, \tag{4}$$

where the mth column $\mathbf{x}_{m,k}$ consists of the past L input samples of the input signal $x_{m,k}$. The scalar $g_m \in \mathbb{C}$ is the mth entry of $\mathbf{g} \in \mathbb{C}^M$, and it may represent an amplitude and phase difference among the M different channels.

In a second example, consider a complex-valued Hammerstein system, as can be seen in Figure 2. Such systems arise, for example, in communication or radar transmitters affected by in-phase and quadrature-phase (IQ) imbalance and/or a nonlinear power amplifier (PA). Assuming the nonlinearity is memory-free and linear in the parameters as

$$u_k = \sum_{m=1}^{M} g_m \varphi_m(x_k), \tag{5}$$

with the input signal x_k, nonlinear functions $\varphi_m(x_k)$, and parameters g_m, the input–output relation of this complex-valued Hammerstein system again can be written in the form of (3). The corresponding input signal matrix results in

$$\mathbf{X}_k = \begin{bmatrix} \varphi_1(x_k) & \cdots & \varphi_M(x_k) \\ \vdots & \ddots & \vdots \\ \varphi_1(x_{k-L+1}) & \cdots & \varphi_M(x_{k-L+1}) \end{bmatrix}. \tag{6}$$

In both applications, the vectors $\mathbf{h} \in \mathbb{C}^L$ and $\mathbf{g} \in \mathbb{C}^M$ can be interpreted as coefficient vectors.

By analyzing (3), it is easy to see that every bilinear model can be rewritten as a linear model as

$$y_k = \mathbf{f}^T \widetilde{\mathbf{x}}_k + n_k, \tag{7}$$

where we denote $\mathbf{f} = \mathbf{g} \otimes \mathbf{h}^* \in \mathbb{C}^{LM}$ as the corresponding linear coefficient vector and $\widetilde{\mathbf{x}}_k = \mathrm{vec}\,[\mathbf{X}_k] \in \mathbb{C}^{LM}$ as the corresponding input vector.

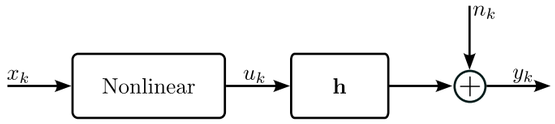


Figure 2: Block diagram of a complex-valued Hammerstein system.

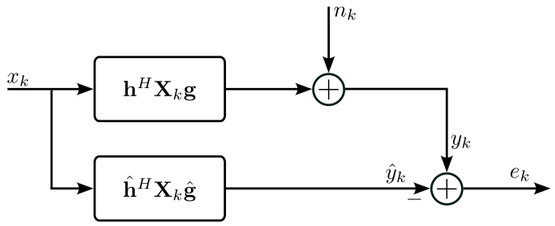


Figure 3: Block diagram of a system identification task using optimum or adaptive filters.

Using optimum or adaptive filters, with their key structure illustrated in Figure 3, the goal is to find filter parameters $\hat{\mathbf{h}} \in \mathbb{C}^L$ and $\hat{\mathbf{g}} \in \mathbb{C}^M$ or $\hat{\mathbf{f}} \in \mathbb{C}^{LM}$ that minimize a cost function based on the error signal e_k. While a bilinear system has $L + M$ unknown parameters, finding $\hat{\mathbf{f}}_k$ directly requires LM parameters to be found. Note that it is only possible to estimate $\mathbf{h}$ and $\mathbf{g}$ up to a complex-valued constant $\nu \in \mathbb{C}$, since

$$\mathbf{h}^H\mathbf{X}_k\mathbf{g} = (\nu\mathbf{h})^H\,\mathbf{X}_k\mathbf{g}\frac{1}{\nu^*}, \tag{8}$$

while $\mathbf{f}$ is unaffected by this scaling factor.

3. COMPLEX-VALUED BILINEAR FILTERS

In the following chapter, several complex-valued bilinear filters are derived. To approximate the output of a system as in (3), we investigate four different methods. First, this can be achieved by using either $2\mathbb{R}$ or $4\mathbb{R}$ bilinear filter structures. Second, a fully complex-valued bilinear filter structure is applied to estimate $\mathbf{h}$ and $\mathbf{g}$. The fourth method is based on the corresponding linear system shown in (7), thus a complex-valued linear filter may be used [37, 38, 42, 43]. However, this may result in slow convergence speeds because LM coefficients have to be estimated instead of $L + M$ in the bilinear case.

It should be noted that $2\mathbb{R}$ bilinear filters and $4\mathbb{R}$ bilinear filters may be interpreted as simple extensions from the vast literature on real-valued bilinear filters [13–24]. Thus, in this work only the derivations of the $2\mathbb{R}$ bilinear LMS ($2\mathbb{R}$-BLMS) filter and the $4\mathbb{R}$ bilinear LMS ($4\mathbb{R}$-BLMS) filter are shown. The derivations of further $2\mathbb{R}$ and $4\mathbb{R}$ optimum and adaptive bilinear filters can be carried out similarly.

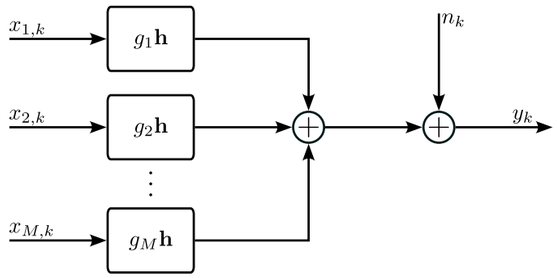


图 1：复值 MISO 系统的框图。

它的结构在很大程度上取决于当前的应用程序。同样，参数向量 $\mathbf{h}$ 和 $\mathbf{g}$ 的物理解释也非常依赖于应用。作为一个介绍性的玩具示例，图 1 中的复值 MISO 系统的输入输出关系可以写成 (3) 的形式。当每个通道脉冲响应是公共脉冲响应 $\mathbf{h}$ 的缩放副本时，该模型有效。将 M 输入信号 $x_{m,k}$ 与 M 线性通道 $g_m\mathbf{h} \in \mathbb{C}^L$, for $m = 1, \ldots, M$ 结合使用，输入信号矩阵定义为

$$\mathbf{X}_k = \begin{bmatrix} \mathbf{x}_{1,k} & \cdots & \mathbf{x}_{M,k} \end{bmatrix}, \tag{4}$$

其中第 m 列 $\mathbf{x}_{m,k}$ 由输入信号 $x_{m,k}$ 过去的 L 输入样本组成。标量 g_m ∈C是$\mathbf{g}$∈ $\mathbb{C}^M$ 的第 m 项，它可以表示 M 不同通道之间的幅度和相位差。

在第二个示例中，考虑一个复值 Hammerstein 系统，如图 2 所示。此类系统出现在受同相和正交相位 (IQ) 不平衡和/或非线性功率放大器 (PA) 影响的通信或雷达发射机中。假设非线性是无记忆的并且参数是线性的：

$$u_k = \sum_{m=1}^{M} g_m \varphi_m(x_k), \tag{5}$$

有了输入信号 x_k、非线性函数 $\varphi_m(x_k)$ 和参数 g_m，这个复值Hammerstein系统的输入输出关系又可以写成(3)的形式。相应的输入信号矩阵结果为

$$\mathbf{X}_k = \begin{bmatrix} \varphi_1(x_k) & \cdots & \varphi_M(x_k) \\ \vdots & \ddots & \vdots \\ \varphi_1(x_{k-L+1}) & \cdots & \varphi_M(x_{k-L+1}) \end{bmatrix}. \tag{6}$$

在这两个应用中，向量 $\mathbf{h} \in \mathbb{C}^L$ 和 $\mathbf{g} \in \mathbb{C}^M$ 可以解释为系数向量。

通过分析(3)，很容易看出每个双线性模型都可以重写为线性模型：

$$y_k = \mathbf{f}^T \widetilde{\mathbf{x}}_k + n_k, \tag{7}$$

其中，我们将 $\mathbf{f} = \mathbf{g} \otimes \mathbf{h}^* \in \mathbb{C}^{LM}$ 表示为相应的线性系数向量，将 $\widetilde{\mathbf{x}}_k = \mathrm{vec}\,[\mathbf{X}_k] \in \mathbb{C}^{LM}$ 表示为相应的输入向量。

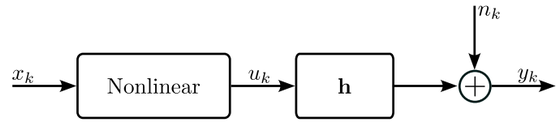


图 2：复值 Hammerstein 系统的框图。

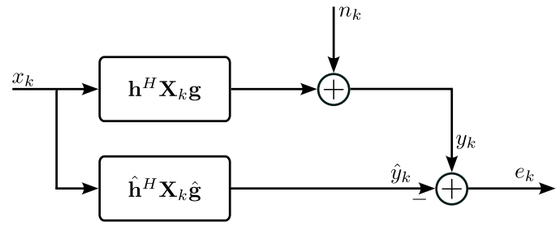


图 3：使用最优或自适应滤波器的系统识别任务的框图。

使用最佳或自适应滤波器（其关键结构如图 3 所示），目标是找到滤波器参数 $\hat{\mathbf{h}} \in \mathbb{C}^L$ 和 $\hat{\mathbf{g}}$ $\in \mathbb{C}^M$ or $\hat{\mathbf{f}} \in \mathbb{C}^{LM}$，以最小化基于误差信号 e_k 的成本函数。虽然双线性系统具有 $L + M$ 未知参数，但查找 $\hat{\mathbf{f}}_k$ 直接需要找到 LM 参数。请注意，只能将 $\mathbf{h}$ 和 $\mathbf{g}$ 估计为复值常数 ν ε$\mathbb{C}$，因为

$$\mathbf{h}^H\mathbf{X}_k\mathbf{g} = (\nu\mathbf{h})^H\,\mathbf{X}_k\mathbf{g}\frac{1}{\nu^*}, \tag{8}$$

而 $\mathbf{f}$ 不受此缩放因子的影响。

3. 复值双线性滤波器

在下一章中，将推导几个复值双线性滤波器。为了近似（3）中的系统输出，我们研究了四种不同的方法。首先，这可以通过使用 $2\mathbb{R}$ 或 $4\mathbb{R}$ 双线性滤波器结构来实现。其次，应用完全复值双线性滤波器结构来估计 $\mathbf{h}$ 和 $\mathbf{g}$。第四种方法基于（7）所示的相应线性系统，因此可以使用复值线性滤波器[37,38,42,43]。然而，这可能会导致收敛速度缓慢，因为在双线性情况下必须估计 LM 系数而不是 $L + M$。

应该注意的是，$2\mathbb{R}$双线性滤波器和$4\mathbb{R}$双线性滤波器可以被解释为来自关于实值双线性滤波器的大量文献的简单扩展[13–24]。因此，在这项工作中仅显示了 $2\mathbb{R}$ 双线性 LMS ($2\mathbb{R}$-BLMS) 滤波器和 $4\mathbb{R}$ 双线性 LMS ($4\mathbb{R}$-BLMS) 滤波器的推导。进一步的 $2\mathbb{R}$ 和 $4\mathbb{R}$ 最优和自适应双线性滤波器的推导可以类似地进行。